Organic Electronics 14 (2013) 1586–1590

Contents lists available at SciVerse ScienceDirect

Organic Electronics

journal homepage: www.elsevier.com/locate/orgel

Letter

Hydrazine-based n-type doping process to modulate Dirac point of graphene and its application to complementary inverter

In-Yeal Lee [a,1], Hyung-Youl Park [a,1], Jin-Hyung Park [a], Jinyeong Lee [b], Woo-Shik Jung [c], Hyun-Yong Yu [d], Sang-Woo Kim [b], Gil-Ho Kim [a,*], Jin-Hong Park [a,*]

[a] School of Electronics and Electrical Engineering, SKKU Advanced Institute of Nanotechnology (SAINT), SKKU-Samsung Graphene Center, Sungkyunkwan University, Suwon 440-746, Republic of Korea
[b] School of Advanced Materials Science and Engineering, SKKU Advanced Institute of Nanotechnology (SAINT), Center for Human Interface Nanotechnology (HINT), SKKU-Samsung Graphene Center, Sungkyunkwan University, Suwon 440-746, Republic of Korea
[c] Department of Electrical Engineering, Stanford University, Stanford, CA 94305, USA
[d] School of Electrical Engineering, Korea University, Seoul 136-701, Republic of Korea

ARTICLE INFO

Article history:
Received 23 October 2012
Received in revised form 11 January 2013
Accepted 13 March 2013
Available online 30 March 2013

Keywords:
Graphene
N-doping
Hydrazine
Inverter

ABSTRACT

In this paper, chemical n-type doping process of graphene using hydrazine monohydrate solution (N_2H_4–H_2O) is demonstrated. This method successfully modulates the Dirac point of pristine graphene by adjusting the concentration of hydrazine solution and also provides an effective n-type doping in graphene. First, the hydrazine treated and pristine graphene films are systematically investigated by Raman and FT-IR spectroscopy. Second, with p- and n-channel FETs fabricated on both pristine and hydrazine treated n-type graphene, complementary graphene inverter is demonstrated.

1. Introduction

Graphene, which is a single atomic layer of graphite, is a very attractive material for post-silicon (Si) electronics because of its unique physical and chemical properties such as extremely high mobility, ballistic electron transport, high mechanical strength, high flexibility and optical transparency [1–3]. Although pristine graphene is known to have theoretically ambipolar property which is desirable in implementing complex logic circuits, it usually works as a p-type material in air because of unexpected impurity problems such as dangling bonds, residual polymers, and oxidized surfaces [4,5]. In order to recover the ambipolar field effect on graphene, hexagonal boron nitride with similar lattice structure to graphene was proposed for the passivation or encapsulation layer [6,7]. On the other side, various graphene doping methods were studied to reduce the unnecessary contamination and to modulate its electronic properties [8–11]. In this letter, we propose a chemical doping method using hydrazine monohydrate solution (N_2H_4–H_2O), which can produce a n-type graphene with Dirac point modulation. In addition, complementary graphene inverter is demonstrated by combining p-channel field effect transistor (FET) fabricated on the pristine graphene and n-channel FET on the hydrazine treated n-type graphene. Although Some et al. [12] recently demonstrated n-type graphene by reducing graphene oxide using hydrazine-based process, this letter's focus is to demonstrate the feasibility of hydrazine-based n-type doping process for (1) the modulation of Dirac point (from p-type to n-type) on pristine graphene and (2) its application to complementary graphene inverter.

* Corresponding authors. Current address: School of Electronics and Electrical Engineering, Sungkyunkwan University, Cheoncheon-dong, Jangan-gu, Suwon-si, Gyeonggi-do 440-746, Republic of Korea. Tel.: +82 31 299 4951.
E-mail addresses: ghkim@skku.edu (G.-H. Kim), jhpark9@skku.edu (J.-H. Park).
[1] These authors contributed equally to this work.

1566-1199/$ - see front matter © 2013 Elsevier B.V. All rights reserved.
http://dx.doi.org/10.1016/j.orgel.2013.03.022

2. Experiments

Fig. 1 shows the fabrication process flow for complementary graphene inverter. Graphene layers were synthesized on copper film by conventional CVD method [5]. The as-grown graphene layers were then transferred on thermally grown 300 nm thick SiO_2 film on heavily n-type Si (0.007–0.02 Ω-cm) substrate by a dry transfer technique. Source/drain (*S*/*D*) regions were defined by optical lithography, and metal electrode of 10 nm Ti and 50 nm Au were formed by electron beam evaporation and lift-off process. In addition, 10 μm by 50 μm active graphene region was defined by lithography and O_2 plasma etching process. For n-channel FET fabrication, the above samples were dipped in 0.05%, 0.5%, and 100% concentrated hydrazine solutions for 15 s and went through a rapid washing process in DI-water. Both pristine and hydrazine treated graphene films were analyzed by Raman and Fourier transform infrared (FT-IR) spectroscopy. Besides, in order to investigate thermal and environmental stability of the graphene films treated by hydrazine, the treated samples were annealed at 90 °C and also exposed in air for different periods time (10, 20, 30, and 40 s for thermal stability analysis/1, 2, 3, 4, 5, 6, 7, and 8 days for the air stability analysis). For complementary graphene inverter fabrication, graphene/SiO_2/highly doped Si substrates with pristine (p-type) and hydrazine treated (n-type) regions were used to make p- and n-channel FETs, respectively. Polydimethylsiloxane (PDMS) layer was partially covered on the graphene p-channel FETs to prevent p-type graphene from converting to n-type during hydrazine treatment. The p- and n-channel FETs were then interconnected using a silver paste. For electrical characterization, drain current–gate voltage (I_D–V_G) and input voltage–output voltage (V_{IN}–V_{OUT}) transfer characteristics were measured in both FETs and inverter. Drain–source voltage (V_{DS}) bias of 1 V was applied to the FETs when measuring the I_D–V_G characteristic.

3. Results and discussion

Fig. 2a shows the Raman spectra of pristine and hydrazine treated graphene films. According to the Raman results, the initially obtained graphene film seems to have a few monolayers indicated by a lower 2D to *G* peak intensity ratio ($I_{2D}/I_G = 0.95$) value than that of a single layer graphene (~2.2) [13]. After performing the n-type doping process by hydrazine, the I_{2D}/I_G value was apparently reduced from 0.95 to 0.68, which a similar phenomenon reported by Li et al. and Sood et al. [11,14] The hydrazine treated graphene film in this work shows lower I_D/I_G value (0.25) than the pristine graphene (0.35), suggesting decrease of defects, although carbon atoms in graphene are normally thought to be in a disordered state by nitrogen doping process [13]. In addition, it was confirmed that this n-type doping process affects the position of *G* and 2D peaks. The G peak of the hydrazine treated graphene was slightly down-shifted to 1577 cm^{-1} from that (1581 cm^{-1}) of the pristine graphene which is thought to be an artifact of defects creation on graphene layer during the molecular doping process [11]. We also observed the 2D peak shift of the hydrazine treated graphene at 2679 cm^{-1}, which is located at higher frequency than that (2664 cm^{-1}) of pristine graphene. This 2D peak shift phenomenon was previously confirmed by Dong et al. in graphene films obtained by n-type and p-type molecular doping methods, and they also concluded that it was attributed to the defect generation by the molecular doping [11]. The n- and p-type doping processes slightly move

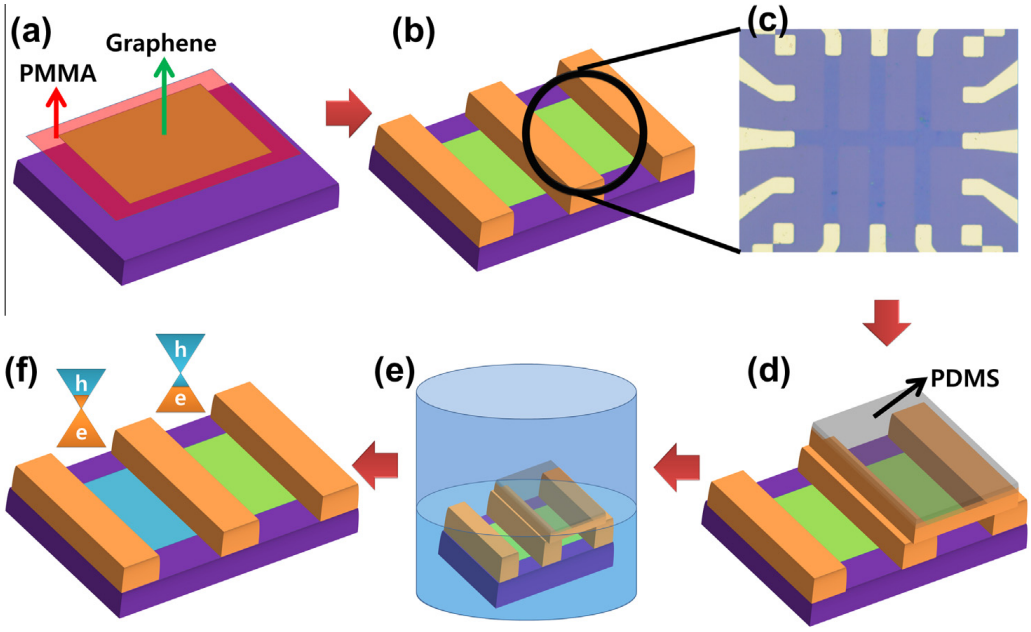

Fig. 1. Fabrication process flow for complementary graphene inverter. (a) Graphene transferred on Si dioxide substrate, (b) Metallization of Ti/Au electrodes and O_2 plasma etching process, (c) optical image of graphene FET, (d) PDMS covered on the graphene p-channel FET, (e) hydrazine treatment, and (f) Complementary graphene invertor fabricated on selectively doped graphene films.

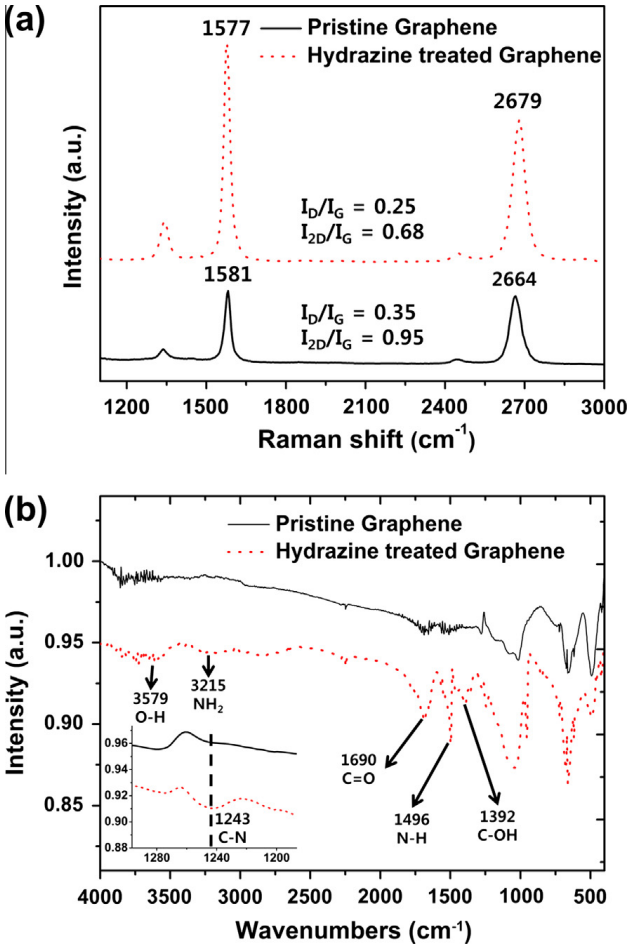

Fig. 2. Raman and FT-IR spectra of pristine and hydrazine treated graphene films.

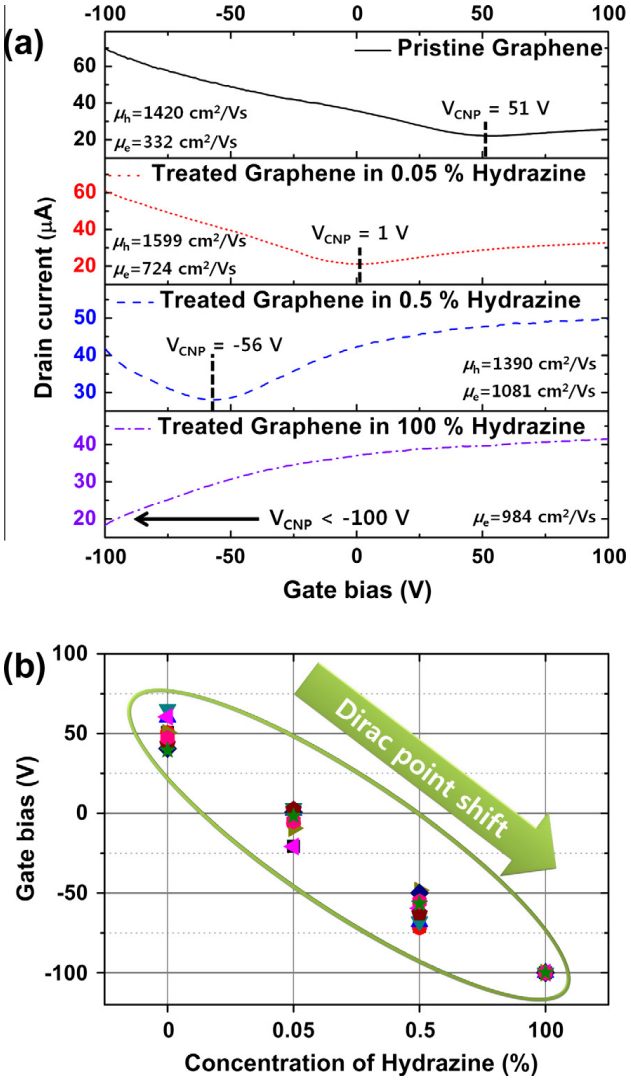

Fig. 3. (a) I_D–V_G characteristics and mobility values of FETs fabricated on the pristine, 0.05% hydrazine treated, 0.5% hydrazine treated, and 100% hydrazine treated graphene films. (b) Dirac points of the FETs as a function of hydrazine concentration.

the 2D peak towards lower and higher frequency regions, respectively. Fig. 2b shows the result of FT-IR spectra showing newly induced functional groups on graphene. After hydrazine treatment, several peaks appeared at 1243, 1392, 1496, 1690, 3215 and 3579 cm^{-1} which indicate C—N stretching vibration, C—OH stretching vibration, N—H in-plane stretch, C=O amide carbonyl stretch, NH_2 stretch, and O—H stretching vibrations, respectively. Especially, the peak at 3215 cm^{-1} confirms that NH_2 molecule, which works as an electron-donating agent [11], is newly bonded to graphene during the hydrazine treatment. However, the intensity of NH_2 stretch peak is relatively low compared to the other peaks, indicating NH_2 molecules are locally and weakly bonded to graphene. Another peak at 1243 cm^{-1} implies carbon bonding with nitrogen atoms, which increases the concentration of free electron carriers [15]. Therefore, it is thought that the hydrazine treatment successfully produced n-type graphene.

In order to re-confirm the validity of graphene n-type doping process, we additionally investigated the electrical properties of the graphene-channel FETs fabricated on the pristine and hydrazine treated graphene films. Fig. 3a shows I_D–V_G characteristics and extracted mobility of the FETs formed on the different graphene films (pristine, 0.05% hydrazine treated, 0.5% hydrazine treated, and 100% hydrazine treated graphene). Mobility of the graphene FETs was extracted by using a drain current equation in a linear transfer regime [16]. The electron mobility was increased from 332 cm^2/V-s to 1081 cm^2/V-s as using a higher concentration hydrazine solution, even though the hole mobility showed a slightly decreasing trend. From these I_D–V_G curves (10 samples in each condition), Dirac points were also extracted and plotted in Fig. 3b. Dirac point of the pristine graphene FET was observed at around +50 V since the pristine graphene generally serves as a p-type material in air because of unexpected impurity problems. However, Dirac points were respectively shifted to 1 V and −55 V after performing 0.05% and 0.5% hydrazine treatment process, indicating that this n-type doping method using hydrazine solution successfully (1) produces n-type graphene and (2) modulates its Dirac point. In the case of 100% hydrazine treated samples, all of Dirac points were not observed in the voltage range (−100 V to 100 V) due to its high n-type doping concentration. As a result,

it was assumed that the value was about −100 V, as seen in Fig. 3b. As mentioned here, another important benefit of this doping method is that it is possible to control the position of Dirac point (in other words, doping concentration) in graphene films by adjusting the concentration of hydrazine solution. Compared to previously reported graphene doping methods through electrochemical reaction with NH_3 gas [8], self-assemble monolayers (SAMs) [9], and a buffered oxide etchant (BOE) treatment [10], this hydrazine-based doping method can not only control the Dirac point but also can be easily performed by just dipping pristine graphene in hydrazine solution for only a few seconds. However, the Dirac point was shifted towards the positive gate biased region with increased annealing time from 10 s to 40 s at 90 °C. Similar effect was also observable with increased air exposure time from 1 day to 8 days. Those phenomena seem to be respectively caused by (1) the detachment of molecules generated by the hydrazine treatment on graphene at 90 °C and (2) the effect of —OH groups introduced from air on the previously formed molecules.

Finally, in order to show the feasibility of hydrazine-based n-type doping process for graphene-based electronic devices, we fabricated a complementary graphene inverter with p- and n-channel FETs formed on pristine and 0.05% hydrazine treated graphene films, respectively. In Fig. 4a, the resistance curve was shifted towards the negative gate voltage regime, meaning that it works as n-channel FET after the hydrazine n-doping process. Since the V_{OUT} of the graphene inverter is given by the relationship $V_{OUT} = -V_{DD}/(1 + R_p/R_n)$, where V_{DD} is 1 V, R_p (or R_n) is resistance of p (or n)-channel FET, and R_p/R_n is a function of V_{IN}, the calculated V_{OUT} decreases between the two Diract points (V_{CNP} = 79 V for p-channel FET and 11 V for n-channel FET) with the increase of V_{IN} [17,18]. As shown in Fig. 4b, experimentally measured voltage transfer characteristic was well fitted to the calculated one. According to the resistance curve in Fig. 4a, p- and n-channel FETs seem to be respectively turned on and off at low V_{IN} region at around 11 V. As a result, 70% of V_{DD} (0.7 V) is observed at the output node. Similarly, in the high V_{IN} region, about 30% of V_{DD} (0.3 V) is shown because p- and n-channel FETs are turned off and on, respectively. Compared to the previous graphene inverters fabricated with n-channel FETs obtained by annealing [17] and gel dielectric [18] techniques, our inverter shows slightly higher difference between high (0.7 V) and low (0.3 V) output voltages. It seems to be caused by the larger difference between Dirac points for graphene n- and p-channel FETs, which was achieved by the hydrazine-based doping process. We also expect that a high–low transition region can be adjusted by modulating the concentration of hydrazine solution and consequently Dirac point of graphene n-FET. We note that V_{OUT} cannot reach zero or V_{DD} value, because graphene-channel FETs cannot be completely turned off due to their low energy band gap.

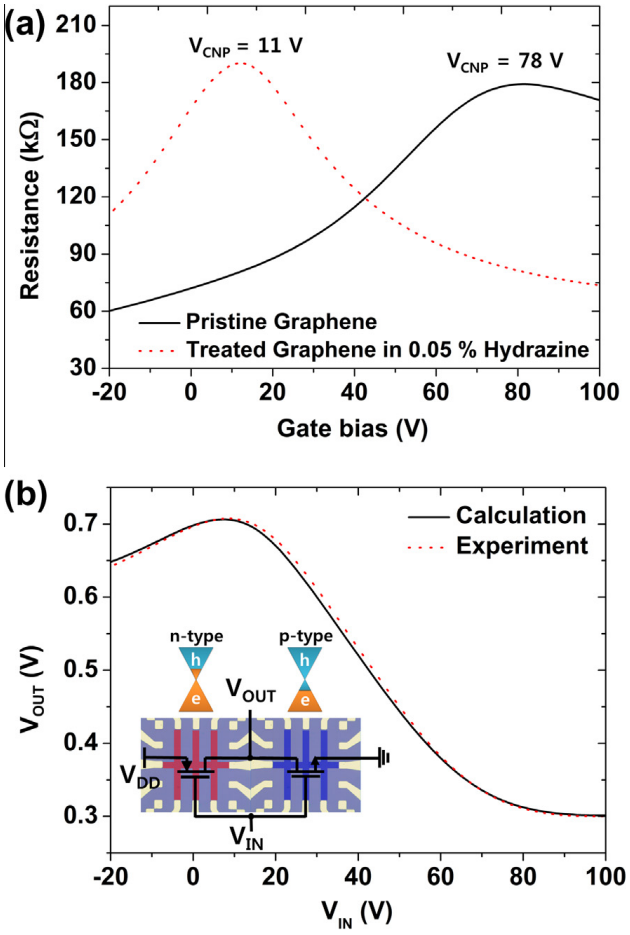

Fig. 4. (a) Resistances as a function of V_G of the p- and n-channel FETs fabricated on the pristine (p-type) and 0.05% hydrazine treated (n-type) graphene films. (b) Calculated and measured voltage transfer characteristics (V_{IN}–V_{OUT}) of the complementary graphene inverter. (b: inset) Optical image and circuit diagram for the graphene inverter.

4. Conclusion

We developed a hydrazine-based chemical n-doping process for graphene, which allows the control of Dirac point in graphene. The feasibility of the n-doping process for graphene-based electronic devices was successfully demonstrated in this letter by fabricating a complementary graphene inverter with p- and n-channel FETs on pristine and hydrazine treated graphene, respectively.

Acknowledgements

This research was supported by (1) Basic Science Research Program through the National Research Foundation of Korea (NRF) funded by the Ministry of Education, Science, and Technology (NRF-2011-0007997) and (2) World Class University program funded by the Ministry of Education, Science and Technology through the National Research Foundation of Korea (R32-10204).

References

[1] A.K. Geim, Science 324 (2009) 1530.
[2] A.K. Geim, K.S. Novoselov, Nat. Mater. 6 (2007) 183.
[3] A.H. Castro Neto, F. Guinea, N.M.R. Peres, K.S. Novoselov, A.K. Geim, Rev. Mod. Phys. 81 (2009) 109.
[4] Y.-J. Kang, J. Kang, K.J. Chang, Phys. Rev. B 78 (2008) 115404.

[5] K.H. Lee, H.-J. Shin, J. Lee, I.-Y. Lee, G.-H. Lee, J.-Y. Choi, S.-W. Kim, Nano Lett. 12 (2012) 714.
[6] C.R. Dean, A.F. Young, I. Meric, C. Lee, L. Wang, S. Sorgenfrei, K. Watanabe, T. Taniguchi, P. Kim, K.L. Shepard, J. Hone, Nat. Nanotechnol. 5 (2010) 722.
[7] A.S. Mayorov, R.V. Gorbachev, S.V. Morozov, L. Britnell, R. Jalil, L.A. Ponomarenko, P. Blake, K.S. Novoselov, K. Watanabe, T. Taniguchi, A.K. Geim, Nano Lett. 11 (2011) 2396.
[8] X. Wang, X. Li, L. Zhang, Y. Yoon, P.K. Weber, H. Wang, J. Guo, H. Dai, Science 324 (2009) 768.
[9] J. Park, S.B. Jo, Y.-J. Yu, Y. Kim, J.W. Yang, W.H. Lee, H.H. Kim, B.H. Hong, P. Kim, K. Cho, K.S. Kim, Adv. Mater. 24 (2012) 407.
[10] D.-W. Shin, H.M. Lee, S.M. Yu, K.-S. Lim, J.H. Jung, M.-K. Kim, S.-W. Kim, J.-H. Han, R.S. Ruoff, J.-B. Yoo, ACS Nano 9 (2012) 7781.
[11] X. Dong, D. Fu, W. Fang, Y. Shi, P. Chen, L.-J. Li, Small 5 (2009) 1422.
[12] S. Some, P. Bhunia, E.H. Hwang, K. Lee, Y. Yoon, S. Seo, H. Lee, Chem. Eur. J. 18 (2012) 7665.
[13] G.-P. Dai, J.-M. Zhang, S. Deng, Chem. Phys. 516 (2011) 212.
[14] A. Das, S. Pisana, B. Chakraborty, S. Piscanec, S.K. Saha, U.V. Waghmare, K.S. Novoselov, H.R. Krishnamurthy, A.K. Geim, A.C. Ferrari, A.K. Sood, Nat. Nanotechnol. 3 (2008) 210.
[15] D. Geng, S. Yang, Y. Zhang, J. Yang, J. Liu, R. Li, T.-K. Sham, X. Sun, S. Ye, S. Knights, Appl. Sur. Sci. 257 (2011) 9193.
[16] B.J. Kim, H. Jang, S.-K. Lee, B.H. Hong, J.-H. Ahn, J.H. Cho, Nano Lett. 10 (2010) 3464.
[17] F. Traversi, V. Russo, R. Sordan, Appl. Phys. Lett. 94 (2009) 223312.
[18] S.-L. Li, H. Miyazaki, A. Kumatani, A. Kanda, K. Tsukagoshi, Nano Lett. 10 (2010) 2357.